



Deposited via The University of York.

White Rose Research Online URL for this paper:

<https://eprints.whiterose.ac.uk/id/eprint/117457/>

Version: Accepted Version

Article:

Pryor, Paul Robert (2017) The Salmonella effector SseJ disrupts microtubule dynamics when ectopically expressed in Normal Rat Kidney cells. PLoS ONE. ISSN: 1932-6203

<https://doi.org/10.1371/journal.pone.0172588>

Reuse

This article is distributed under the terms of the Creative Commons Attribution (CC BY) licence. This licence allows you to distribute, remix, tweak, and build upon the work, even commercially, as long as you credit the authors for the original work. More information and the full terms of the licence here:

<https://creativecommons.org/licenses/>

Takedown

If you consider content in White Rose Research Online to be in breach of UK law, please notify us by emailing eprints@whiterose.ac.uk including the URL of the record and the reason for the withdrawal request.

1 The *Salmonella* effector SseJ disrupts microtubule dynamics when ectopically
2 expressed in Normal Rat Kidney cells.

3

4 Sally A Raines¹, Michael R. Hodgkinson¹, Adam A. Dowle³ and Paul R
5 Pryor^{1,2*}

6

7

8

9

10 ¹Department of Biology and ²Hull York Medical School, Wentworth Way,
11 University of York. York. YO10 5DD. United Kingdom.

12 ³Technology Facility, Department of Biology, Wentworth Way, University of
13 York. York. YO10 5DD. United Kingdom

14 *Correspondence: paul.pryor@york.ac.uk

15

16 Short title: SseJ disrupts microtubules

17

18 **Abstract**

19 *Salmonella* effector protein SseJ is secreted by *Salmonella* into the host cell
20 cytoplasm where it can then modify host cell processes. Whilst host cell small
21 GTPase RhoA has previously been shown to activate the acyl-transferase
22 activity of SseJ we show here an un-described effect of SseJ protein
23 production upon microtubule dynamism. SseJ prevents microtubule collapse
24 and this is independent of SseJ's acyl-transferase activity. We speculate that
25 the effects of SseJ on microtubules would be mediated *via* its known
26 interactions with the small GTPases of the Rho family.

27 **Introduction**

28 *Salmonellae* are gram-negative bacteria that can infect a wide range of
29 hosts and in humans can cause diseases such as typhoid fever and
30 gastroenteritis. There are ~2600 recognized *Salmonella* serovars of which
31 over half are represented by *S. enterica* subspecies *enterica* (*S. enterica*
32 subspecies I), constituting 99% of human
33 clinical *Salmonella* infections. *Salmonella enterica* serovar Typhimurium (*S.*
34 Typhimurium; the cause of gastroenteritis) uses two type III secretion systems
35 (T3SS) to translocate pathogen effector proteins directly into the host cell's
36 cytoplasm. (reviewed by [1]). The T3SS encoded by *Salmonella* pathogenicity
37 island-1 (SPI-1; T3SS-1) is mostly active when extracellular *Salmonella* come
38 into contact with a host cell and allows effector proteins to be translocated
39 directly into the cell cytoplasm and causes the bacteria to be actively
40 phagocytosed. Another T3SS encoded by *Salmonella* pathogenicity island-2
41 (SPI-2; T3SS-2) enables the bacteria to multiply intracellularly in a *Salmonella*

42 containing vacuole (SCV) by allowing further effector proteins to be
43 translocated directly from the *Salmonella* (through the phagosomal
44 membrane) into the host cell cytoplasm. It is unclear precisely how
45 *Salmonella* uses its multiple T3SS effector proteins to survive intracellularly
46 but theories range from delaying fusion with the degradative organelle the
47 lysosome [2], though the role of the T3SS in this process is contested [3], to
48 preventing the delivery of lysosomal hydrolases to the *Salmonella*-containing
49 phagosomal compartment by altering mannose 6-phosphate receptor
50 trafficking [4]. Only a finite number of intracellular membrane trafficking and
51 signalling events can be manipulated by a pathogen and hence successful
52 intracellular pathogens are often found to target the same host cell molecules,
53 for instance phosphoinositides are targeted by both *Salmonellae* and
54 *Mycobacteria* [5, 6]. Understanding how *Salmonella* survives intracellularly not
55 only provides information about *Salmonella* pathogenesis but potentially what
56 processes may also be targeted by other intracellular pathogens.

57 To understand the role of *Salmonella* T3SS effector proteins in the flow
58 of membranes to the lysosome a rapid screen was undertaken in
59 *Saccharomyces cerevisiae* (*S. cerevisiae*). Membrane trafficking events are
60 conserved between yeast and mammalian cells. Therefore, yeast can be used
61 to rapidly identify any *Salmonella* proteins that alter membrane traffic to the
62 yeast vacuole, the equivalent of the mammalian lysosome. The screen
63 identified the *Salmonella* virulence protein SseJ and subsequently we show a
64 previously un-described effect of this protein on the stability of host cell
65 microtubules. Microtubules are required for phagosome fusion [7-9] and by
66 promoting a network of stable microtubules this can aid in phagosome fusion

67 with endocytic organelles enabling nutrients to be delivered to the
68 phagosomal lumen, promoting bacterial replication.

69

70 **Results**

71 **SseJ production causes membrane trafficking defects**

72 To identify *Salmonella* proteins that can disrupt intracellular membrane
73 trafficking, a genomic library from *Salmonella* was generated and the DNA
74 inserted into a yeast expression vector. *S. cerevisiae* were then transformed
75 with the plasmid library and colonies screened for a defect in the delivery of
76 the vacuolar hydrolase, carboxypeptidase-Y (CPY), to the yeast vacuole. If
77 there is disruption of CPY delivery to the vacuole then CPY is secreted. We
78 assayed the secretion of a CPY-invertase fusion protein that oxidises an
79 applied solution of o-diansidine to a brown precipitate [10]. This approach has
80 been successfully employed to identify effector proteins of *Legionella*
81 *pneumophila* [11] and *Mycobacterium tuberculosis* [12] that interfere with
82 yeast membrane trafficking. Yeast transformed with the plasmid library were
83 screened for CPY-Inv secretion and 8 yeast clones were found to have CPY-
84 Inv secretion in a plasmid dependent manner. One of the clones identified a
85 6kb fragment of *Salmonella* chromosomal DNA containing 1 partial open
86 reading frame (ORF) and 6 complete ORFs (Fig 1A). All of the *Salmonella*
87 genes identified in the plasmid, were cloned and expressed individually in
88 yeast and re-assayed for CPY secretion. Qualitative CPY-Inv secretion on
89 agar plates showed that SseJ caused CPY secretion, though we did not
90 analyse the protein production levels of the other 5 proteins. (Fig. 1B).

91 Quantitative CPY-Inv secretion from yeast in liquid culture demonstrated that
92 SseJ dependent CPY-Inv secretion was equivalent to that in yeast lacking the
93 CPY receptor, VPS10 (Δ VPS10; fig. 1C). There are numerous intermediate
94 vesicles involved in delivery of CPY to the vacuole and the retrograde
95 trafficking of the VPS10 receptor. When CPY is secreted, due to a trafficking
96 defect, it is possible to examine the phenotype of the yeast vacuole and in
97 some cases determine which part of the trafficking step of CPY from the Golgi
98 to the vacuole is disrupted [13, 14]. Using the membrane dye FM4-64 to label
99 the yeast vacuole in yeast expressing SseJ, no differences in the morphology
100 of the vacuole were seen compared to wild-type yeast (fig. 1D). These data
101 indicated that SseJ alone can cause a membrane trafficking defect in yeast.

102 **SseJ production re-distributes late endocytic organelles**

103 SseJ is one of several virulence proteins secreted by *Salmonella*'s T3SSs into
104 the host's cytoplasm directly from the bacteria [15]. *Salmonella* strains lacking
105 SseJ are attenuated in replication [16-19] indicating that SseJ is crucial for
106 bacterial intracellular replication. SseJ was then expressed in mammalian
107 cells. In this case, we used Normal Rat Kidney (NRK) cells since they show
108 good spatial resolution between endocytic vesicles and in particular between
109 late endosomes and lysosomes. Late-endocytic organelles are poorly
110 resolved by light microscopy in HeLa cells, which are often used for
111 *Salmonella* infection studies. Constitutive protein production of SseJ was
112 found to cause cell death so myc-tagged SseJ (myc-SseJ) was expressed
113 under the control of a metallothionein promoter allowing for inducible *sseJ*
114 expression upon the addition of cadmium. Immunofluorescence demonstrated
115 that myc-SseJ localises to lysosomes (Fig. 2A) as has previously been

116 reported [19]). Moreover there was a dramatic re-distribution of late endocytic
117 organelles with both late endosomes and lysosomes becoming less peri-
118 nuclear and more peripherally distributed (Fig. 2B). The *trans*-Golgi marker
119 TGN38 was observed to occupy a larger area of the cell (Fig. 2B), but in
120 general cells were flatter with an increased surface area (on average the cell
121 surface area went from 591 μm^2 to 2,057 μm^2 upon SseJ expression). Ectopic
122 SseJ protein production can cause globular membranous compartments
123 (GMCs) [19] and indeed when *sseJ* expression was induced for 24 h,
124 lysosomes were seen to aggregate as observed by LGP120 (rat equivalent of
125 LAMP1) staining (Fig. 2C). The metallothionein promoter regulating *sseJ*
126 expression is slightly leaky due to the presence of trace amounts of heavy
127 metals in the tissue culture media, which explains why the lysosomes are
128 partially aggregated in transfected cells before cadmium addition (Fig. 2C
129 panel b). The re-distribution of organelles is observed when the cytoskeleton
130 is perturbed [20] and indeed when the microtubule polymerisation inhibitor
131 nocodazole was added to cells, late endocytic organelles re-distributed in a
132 manner similar to that observed with SseJ expression (Fig. 2D).

133 **SseJ alters microtubule dynamics**

134 To assess whether the re-distribution of organelles was related to changes to
135 the cytoskeleton the microtubules were visualised in cells expressing SseJ or
136 a mutant SseJ (SseJ S151A). SseJ has homology to the GDSL-like lipolytic
137 enzyme family [21] and shows deacylase, phospholipase and
138 glycerophospholipid-cholesterol acyltransferase (GCAT) activity [22-24].
139 Ser151 in SseJ is the middle serine in a GDSL motif, which is present in
140 GCAT enzymes and mutation of this residue reduces SseJ's deacylase

141 activity by 5 fold [22]. SseJ-S151A still localises to the *Salmonella* containing
142 vacuole and *Salmonella* induced filaments (Sifs) [25] are still visible in a SseJ-
143 S151A mutant strain but the bacteria show reduced virulence [22]. The
144 microtubules, in both WT and mutant-SseJ expressing cells, became
145 disorganised with no clear microtubule organising centre (MTOC; Fig. 3A). In
146 J774.2 macrophages the majority of cells don't have clear microtubules
147 emanating from a MTOC unless they have flattened out on the culture vessel
148 surface (Fig. 3B). Co-cultures of bacteria and J774.2 macrophages causes
149 the macrophages to flatten out and under these conditions the microtubule
150 network becomes more visible. However, a loss of organised microtubules,
151 emanating from a clearly defined MTOC, was seen in mouse macrophages
152 infected with WT *Salmonella* but not in cells infected with Δ sseJ *Salmonella*
153 (Fig. 3B). Typically, Δ sseJ *Salmonella* induced a four-fold increase in visible
154 microtubules emanating from the MTOC compared to control cells, but WT
155 *Salmonella* only induced a two-fold increase (Fig. 3B). Unlike nocodazole that
156 completely disrupts tubulin polymers (Fig. 2D), cells expressing SseJ still
157 show some tubulin polymers albeit in a dis-organised manner. Long-lived,
158 stable microtubules are de-tyrosinated, resulting in the exposure of a
159 glutamate residue (Glu-tubulin), and acetylated [26, 27]. Cells were then
160 examined for the presence of Glu-tubulin (Fig. 3C). In cells expressing both
161 WT and mutant SseJ protein there was a reduction in Glu-tubulin
162 immunolabelling compared to control cells. Furthermore, there was a
163 reduction in acetylated-tubulin (Fig. 3D) in WT and mutant sseJ expressing
164 cells. The reduction in acetylated-tubulin corresponded to the time of induction
165 of sseJ expression (Fig. 3E). SseJ protein production was induced with 10 μ M

166 cadmium and the metal can alter the cytoskeleton [28, 29] but we saw no
167 effect of cadmium on the cytoskeleton in NRK cells without *ssej* expression
168 (all control cells in figure 3 are in the presence of 10 μ M cadmium chloride).
169 Together these data suggested that long-lived microtubules had been de-
170 stabilised in cells expressing SseJ, but some un-organised microtubules could
171 still be observed. When cells were transfected with a plasmid encoding GFP-
172 CLIP-170, a protein that binds to the growing ends of microtubules, and
173 visualised by live cell microscopy, no CLIP-170 movement could be observed
174 in cells expressing SseJ (supplemental movie) compared to control cells
175 (supplemental movie). Similar data were obtained with EB3-tdTomato,
176 another microtubule plus-end binding protein, and single images of EB3-
177 tdTomato transfected cells show the EB3 on the end of microtubules in control
178 cells but no visible incorporation of the EB3 onto microtubules in cells
179 expressing SseJ (Fig 3F). So whilst there was a reduction in long-lived
180 microtubules, as assessed by Glu-tubulin and acetylated-tubulin, there was no
181 dynamism in the remaining microtubules.

182 **SseJ binds both RhoA and RhoC**

183 Rho proteins are small GTPases that are primarily associated with modifying
184 the actin cytoskeleton, but they can effect cell polarity and microtubules [30].
185 SseJ can interact with both RhoA or RhoC [31, 32], with GTP-bound RhoA
186 activating SseJ's lipase activity [32]. SseJ has only previously been shown to
187 bind RhoA or RhoC separately. Large scale immunoprecipitations of SseJ
188 from cells overexpressing SseJ identified both RhoA and RhoC having bound
189 to SseJ under experimental conditions where the GTPases were in their GDP-
190 bound form (Fig. 4A), with WT and SseJ-S151A binding Rho proteins with

191 equal ability (Fig. 4B). These experiments indicate that SseJ can bind either
192 RhoA or RhoC in the presence of each other when neither protein is in a
193 limiting amount. Although we have no evidence, it is unlikely that SseJ is
194 binding both RhoA and RhoC simultaneously. Using an ELISA we found, as
195 has been reported [32], that SseJ did not increase the levels of activated
196 (GTP-bound) RhoA (Fig. 4C).

197 **Discussion**

198 In this study, we aimed to understand how *Salmonella* can survive
199 intracellularly by uncovering *Salmonella* effector molecules that can
200 manipulate membrane trafficking events. Manipulation of membrane traffic
201 may disrupt late-organelle biogenesis, including lysosomes, and therefore
202 provide conditions that enable the bacteria to replicate. We hypothesised that
203 a *Salmonella* T3SS effector molecule may manipulate membrane trafficking in
204 yeast to the same extent as mammalian cells given that the delivery of
205 molecules to the vacuole/lysosome are conserved. Using an unbiased screen
206 we identified SseJ, which is a T3SS effector protein, that caused a membrane
207 trafficking defect in yeast (Fig. 1). This is the first demonstration that SseJ
208 causes changes to membrane trafficking in eukaryotes. The powerful yeast
209 screen led us to examine the distribution of organelles in mammalian cells,
210 expecting them to be perturbed. Indeed, organelles no longer localised to the
211 MTOC (Fig. 2) and this observation could be related to changes to the
212 microtubules (Fig. 3). We further showed that SseJ can bind to both RhoA
213 and RhoC and whilst others have shown that RhoA can regulate the GCAT
214 activity of SseJ [32] this is the first report to prove the hypothesis that SseJ
215 alters the cytoskeleton [33].

216 How might SseJ alter the cytoskeleton? Whilst Rho proteins are well
217 known to alter the actin cytoskeleton they can also alter the stability of
218 microtubules via Diaphanous-related formins (DRFs) [34]. RhoA-mDia1/2 can
219 stimulate microtubule stabilisation with an increase in Glu-tubulin, precisely
220 how this is achieved is unknown, and it is possible that if SseJ recruits active
221 Rho proteins to the lysosome then the RhoA-mDia1/2 balance may be
222 disrupted leading to changes in the microtubules. Whilst we did not observe
223 an increase in Glu-tubulin we did see static microtubules. Although the
224 binding of SseJ to RhoA or RhoC has been documented, our data show for
225 the first time that SseJ can bind RhoA or RhoC when both proteins are
226 present and neither are in limited amounts i.e. SseJ does not preferentially
227 bind RhoA and then RhoC (Fig 4). This does raise the possibility that SseJ
228 may have differential effects through both RhoA and RhoC, with differences
229 between RhoA, RhoB and RhoC well documented [35]. So whilst RhoA-GTP
230 can stimulate the GCAT activity of SseJ [32], the binding of RhoC to SseJ
231 may affect the microtubules. RhoC is reported to have a higher affinity for the
232 kinases Rho-associated coiled-coil containing kinases (ROCK) and Citron
233 kinase compared to RhoA [35]. MAP2/Tau proteins stabilise microtubules and
234 inhibit depolymerisation (reviewed by [36]), an effect seen in SseJ expressing
235 cells, and MAP2/Tau proteins can be phosphorylated by numerous kinases
236 including ROCK [35, 37]. The effects of MAP2/Tau phosphorylation are yet to
237 be determined, but there is a precedence for microtubule regulation by Rho
238 proteins via DRFs and kinases such as ROCK [38]. Expression of *sseJ* before
239 *Salmonella* infection reduces Sif formation [19], which can be explained by the
240 fact that a dynamic cytoskeleton is required for phagosome maturation [39].

241 Additionally, whereas SseJ-S151A has reduced GCAT activity [22] the effects
242 on the microtubules are still seen in the S151A mutant suggesting that the
243 GCAT activity is separate from the microtubule effect, though we can't rule out
244 that there is still enough residual GCAT activity in cells over-expressing *sseJ*.

245 SseJ has been shown to interact indirectly with another T3SS effector
246 protein, SifA [31]. Δ *sifA* mutants escape the phagosomal vacuole but not if a
247 double *sifA sseJ* mutant is made, implying that loss of the integrity of the
248 phagosomal membrane is dependent on SseJ [19]. SifA and SseJ are
249 sufficient to cause endosome tubulation [31] and certainly SifA is required for
250 endosome tubulation [40, 41]. With SifA found to bind to RhoA, and SKIP,
251 which is a kinesin binding protein, it was hypothesised that RhoA, SseJ, SifA
252 and SKIP regulates endosome tubulation along microtubules [31]. However,
253 studies have shown that Δ *sseJ Salmonella* show endosomal tubulation
254 implying that SseJ is dispensable for endosome tubulation in a background
255 where all the other secreted effector proteins are expressed [42, 43].

256 *Salmonella* induced endosomal tubules or *Salmonella* induced
257 filaments (Sifs) are initially dynamic but become stabilised (>8h after cell
258 infection; [42] and this stabilisation could correspond to the changes that we
259 see in the dynamics of the microtubules, given that SseJ is secreted from
260 *Salmonella* within 4 h [17]. It is has been known for a long time that
261 lysosomes can form tubules [44, 45] and that microtubules regulate the
262 distribution of lysosomes [46] and their tubular morphology [7]. Although SseJ
263 is dispensable for the formation of Sifs in infected cells, SseJ may aid in
264 stabilising the Sifs that do form.. Why would this be advantageous to the
265 *Salmonella*? Endosome fusion and delivery of endocytosed material to

266 lysosomes can occur at the end of lysosome tubules [47] and the curvature of
267 the membrane at the tip of a tubule is likely to be more fusogenic with
268 endocytic vesicles compared to a larger, more-rounded phagosomal
269 membrane [48]. By reducing microtubule de-polymerisation this allows
270 *Salmonella* to promote tubular lysosomes (endosomal tubules), in conjunction
271 with other proteins such as SifA, increasing fusion events with endosomal
272 vesicles carrying in nutrients from the extracellular environment. Rho
273 GTPases are a common target of bacterial pathogens [49, 50] and further
274 work is required to determine whether SseJ's effect on cellular microtubules is
275 mediated through RhoA or RhoC.

276 **Materials and Methods**

277 **Reagents and Antibodies**

278 Chemical reagents were of laboratory grade. Anti-c-myc (9E10) antibodies
279 were purified from 9E10 hybridoma tissue culture supernatants
280 (Developmental Studies Hybridoma Bank). Anti rat LGP110 (580), anti-mouse
281 cation-independent mannose 6-phosphate receptor (MPR; 1001) and anti-rat
282 TGN38 (2F7.1) were kind gifts from J. P. Luzio (University of Cambridge, UK).
283 Anti α -tubulin (T-9026) was from Sigma, anti-glu-tubulin was from Synaptic
284 Systems, anti-acetylated tubulin (D20G3), rabbit monoclonal anti-RhoA
285 (67B9) and anti-RhoC (D40E4) were from Cell Signalling.

286 **Yeast Strains**

287 BHY10 and BHY11 haploid yeast strains expressing CPY-Inv [51] and BHY10
288 Δ VPS10::TRP1 were a kind gift from Dr. M. Seaman (University of

289 Cambridge). For the screen BHY10 and BHY11 were mated on YPD agar
290 plates, diploid yeast (BHY12) picked from SC–Lys,-Ade plates and then
291 maintained on YPD agar plates.

292 ***Salmonella* genomic library generation**

293 Chromosomal DNA was isolated from stationary phase *Salmonella*
294 Typhimurium strain 14028 [52]. DNA was partially digested with Sau3AI for 1h
295 at 37°C. DNA was electrophoresed on a gel, and the region corresponding to
296 ≈0.8-5 kb was excised and the DNA purified. pVT-100 U [53] a gift from Dr. K.
297 Bowers (UCL, UK), was linearised with BamHI and then de-phosphorylated
298 using calf intestinal phosphatase. DNA was ligated into linearised pVT-100U
299 using T4 DNA ligase and transformed into NEB 10-beta competent *E.*
300 *coli* (High Efficiency). Ampicillin-resistant colonies (≈0.5x10⁶) were scraped,
301 and plasmid DNA prepared (Qiagen midiprep).

302 **Constructs**

303 SseJ was cloned from *S. Typhimurium* DNA by PCR. Primers were used to
304 append a myc-tag to the SseJ PCR product along with 15bp regions of
305 homology to the destination vector to allow for homologous recombination
306 using In-Fusion cloning (Invitrogen). The myc-tagged SseJ DNA was inserted
307 into the HindIII restriction enzyme site of the ΔpMEP4 vector [54] by
308 homologous recombination. The S151A mutant was made by QuikChange
309 site-directed mutagenesis (Stratagene) of the myc-SseJ construct as per the
310 manufacturer's instructions.

311

312 **Invertase (Inv) assays**

313 The *Salmonella* plasmid library was transformed into BHY12 yeast [55], and
314 transformants were plated on synthetic complete medium without uracil (SC-
315 Ura) plates with 2% (w/v) fructose. Carboxypeptidase-Y-invertase (CPY-Inv)
316 assay, both quantitatively and qualitatively, is based on previous
317 methodologies [10].

318 **FM4-64 Staining**

319 1ml of log-phase yeast were pelleted and then resuspended in 50 μ l YPD
320 medium containing 40 μ M FM 4-64 (Molecular Probes). Yeast were incubated
321 at 30°C for 15 min before the yeast were pelleted and washed with YPD
322 media. Yeast in fresh YPD were then incubated for 30 min at 30°C. Yeast
323 were pelleted and then resuspended in 1ml of H₂O and then aliquots directly
324 visualised by confocal microscopy.

325 **Tissue culture and cell transfection**

326 All cells were cultured in Dulbecco's Modified Eagle's Medium (DMEM),
327 supplemented with 10% (v/v) FCS, 100U/L penicillin, 100mg/L streptomycin
328 and 2mM L-glutamine, in a humidified atmosphere with 5% CO₂. Cells were
329 transfected with plasmid DNA using Fugene 6 (Roche Diagnostics) as per the
330 manufacturer's instructions. Δ pMEP4 transfected cells were selected with
331 media containing 0.2 mg/ml hygromycin to generate a stable population of
332 transfected cells and individual clones were selected and assessed for SseJ
333 protein production. SseJ production was induced with 10 μ M CdCl₂ for 16-24h
334 before analyses.

335 **J774.2 *Salmonella* infection.**

336 J774.2 cells were seeded onto glass coverslips and cultured for 48 h in
337 antibiotic-free DMEM medium supplemented with 10 % (v/v) FBS (heat
338 inactivated to 56 °C for 30 min) and 2 mM glutamine. *Salmonellae* (WT and
339 Δ SseJ *Salmonella enterica* serovar *Typhimurium* strain 12023 were a kind gift
340 from Prof. David Holden, Imperial College London). were cultured overnight in
341 LB media with shaking at 30 °C. An appropriate number of bacteria were
342 taken to infect J774.2 cells at an MOI (multiplicity of infection) of 10 and
343 resuspended in PBS. Bacteria were centrifuged onto cells at 80 x g for 5 min
344 and incubated for 1 h at 37 °C to allow phagocytosis of bacteria. Monolayers
345 were rinsed 3 times with DMEM to remove unbound bacteria, and the media
346 replaced with DMEM containing 150 µg/ml gentamycin to kill extracellular
347 bacteria. The cells were cultured for a further hour, and washed with PBS.
348 The media was then replaced with DMEM containing 10 µg/ml gentamycin,
349 and cells cultured for 24 h to allow intracellular bacteria to grow. Cells were
350 fixed with 4 % formaldehyde in PBS for 20 min at room temperature and then
351 processed for immunofluorescence.

352 **Immunofluorescence**

353 Cells were fixed with 4 % (w/v) formaldehyde in PBS for 20 min at 20°C. Cells
354 to be immunolabelled for microtubules were rinsed with microtubule stabilising
355 buffer (MTSB; 80mM PIPES, pH 6.8, 1mM MgCl₂, 4mM EGTA) then
356 incubated in MTSB containing 0.05% (w/v) saponin (Sigma S-4521) for 1 min
357 then fixed with 2% (w/v) formaldehyde, 0.05% (w/v) glutaldehyde in MTSB for
358 20 min. Cells immunolabelled for Glu-tubulin were fixed with -20°C MeOH for

359 5 min at -20°C. All fixed cells were incubated for 10 min in 50 mM NH₄Cl in
360 PBS followed by 10 min in 0.2 % (w/v) BSA in PBS containing 0.5% (w/v)
361 saponin (PBS-BS). Cells were immunolabelled with primary antibodies in
362 PBS-BS for 1h at 20°C. Cells were rinsed 3 x 5 min with PBS-BS and then
363 incubated with fluorescent secondary-antibodies in PBS-BS for 30 min at
364 20°C. Cells were rinsed 3 x 5 min with PBS-BS before being mounted in
365 Mowiol. Fluorescence was imaged using a Zeiss LSM510 confocal
366 microscope. All images are maximum intensity z-projections unless otherwise
367 stated.

368 **Cell lysates**

369 Lysates were generated by rinsing cells with PBS and then scraping cells into
370 ice cold lysis buffer (150 mM NaCl, 20 mM Tris, pH 8.0, 2 mM EDTA, 0.5 %
371 (v/v) NP-40). Lysates were left on ice for 10 min before removal of detergent
372 insoluble material by centrifugation (16,400 g, 10 min, 4°C).

373 **Immunoprecipitation**

374 9E10 antibody was coupled to Amino Link Plus resin (Pierce) following the
375 manufacturer's instructions. Small scale immunoprecipitations used 20 µl of
376 resin and 250µg of cell lysate and samples were incubated for 2 h at 4°C with
377 rotation. Resins were washed 3 x with lysis buffer and immunoprecipitated
378 proteins eluted using IgG gentle elution buffer (Pierce) and analysed by SDS-
379 PAGE. Large scale immunoprecipitations used 12 x T75 flasks and 2ml of
380 anti-myc resin.

381 **Mass spectroscopy**

382 Proteins in gel bands were reduced with DTT and alkylated with
383 iodoacetamide before digestion with modified porcine trypsin
384 (Promega). Digests were dissolved in 4-hydroxy- α -cyano-cinnamic acid and
385 analysed by positive-ion MALDI-MS/MS using a Bruker ultraflex III. Spectra
386 were submitted to Mascot MS/MS ions search against the NCBI database.

387 **RhoA activity assays**

388 Active RhoA in cell lysates was assessed by ELISA using a RhoA activity
389 assay (RhoA G-LISA; Cytoskeleton, Inc) as per the manufacturer's
390 instructions.

391 **Live cell imaging**

392 NRK cells (WT) or expressing SseJ were transfected with either GFP-
393 CLIP170 (kind gift of Folma Buss, University of Cambridge) or EB3-tdTomato
394 (a kind gift from Dr Anne Straube, University of Warwick) and 24 hours later
395 imaged on an Andor Spinning Disc Confocal Microscope. Images were
396 collected with 200ms exposures and a 800ms delay between exposures,
397 giving 1 frame per second.

398

399

400

401

402

403 **Acknowledgements**

404 We thank Gareth Evans, Nia Bryant, Jonathan Bennett and Nathalie Signoret
405 for helpful advice and for reading the manuscript.

406 **Author Contributions**

407 S.A.R. and M.H. provided technical support and carried out some of the
408 experiments. A.A.D carried out the proteomic identification of proteins. P.R.P
409 designed and carried out the majority of the research and wrote the
410 manuscript.

411

412

413 **Figure Legends**

414 **Figure 1. Expression of *ssej* causes CPY-Inv to be mis-sorted in**
415 ***Saccharomyces cerevisiae*.** (A) Fragment of the *Salmonella* chromosome
416 inserted into the yeast expression vector causing CPY-Inv secretion. (B)
417 Qualitative CPY-Inv secretion in yeast expressing individual *Salmonella* genes
418 identified in (A). Negative control yeast (ctrl) contain just the cloning vector
419 (pVT-100U) and positive control yeast lack the receptor VPS10 for CPY
420 (Δ VPS10). (C) Quantitative CPY-Inv secretion in yeast expressing *Salmonella*
421 genes. Controls as in (B). Data are from n=3-9 (number of experiments for
422 each condition in parentheses above each bar) and are mean \pm S.D.
423 *P<0.001 SseJ c.f. Ctrl (P>0.05 SseJ c.f. Δ VPS10). (D) Fluorescence
424 visualisation of the yeast vacuole in wild type yeast (WT) transformed with
425 vector (pVT-100U) alone or SseJ in pVT-100U (SseJ). Top panels DIC and
426 bottom panels FM 4-64 fluorescence. Scale bar = 10 μ m.

427 **Figure 2. Re-distribution of late endocytic organelles in cells expressing**
428 **SseJ.** (A) NRK cells expressing myc-SseJ were double labelled with anti-myc
429 (a) and anti-lysosome glycoprotein 110 (Lgp110; b) followed by fluorescently
430 labelled secondary antibodies. Panel c is the merged image of panels a and b,
431 co-localisation is shown by yellow. (B) Control (Ctrl) NRK cells or NRK cells
432 expressing myc-SseJ (myc-SseJ) were immuno-labelled for the mannose 6-
433 phosphate receptor (MPR), Lgp110 and *trans*-Golgi network 38 (TGN38)
434 followed by fluorescently-labelled secondary antibodies to visualise the late
435 endosomes, lysosomes and *trans*-Golgi network respectively. (C) Aggregation
436 of Lgp110 in NRK cells expressing SseJ for 24h (a). Quantification of cells

437 showing aggregated lysosomes after induction of SseJ production with
438 cadmium (Cd) (b). Expression of myc-SseJ protein +/- Cd is shown by the
439 western blot insert (b). (D) NRK cells were immunolabelled for microtubules
440 (α -tubulin; a,d), lysosomes (lgp120;b,e) and late endosomes (cation-
441 independent mannose 6-phosphate receptor; c,f) in control cells (ctrl) or after
442 cells had been treated with 10 μ M nocodazole for 1h. Scale bars represent
443 10 μ m.

444 **Figure 3. Microtubules are disrupted in cells expressing SseJ.** (A) Control
445 (Ctrl) NRK cells and cells expressing myc-SseJ (SseJ) or myc-SseJ-S151A
446 (S151A) were fixed and the microtubules visualised using anti α -tubulin
447 antibodies and fluorescently-labelled secondary antibodies. Bars = 10 μ m. (B)
448 J774.2 mouse macrophages were either uninfected (Ctrl) or infected with WT
449 or Δ sseJ *Salmonella* Typhimurium for 24h before fixing. The DNA (blue) was
450 visualised using DAPI and the microtubules (red) were visualised as in A.
451 Bars = 20 μ m. Quantification of the number of cells showing an organised
452 microtubule network under each condition is shown (n=1, scoring 100 cells
453 per condition). (C) Cells as in A were fixed and de-tyrosinated α -tubulin (Glu-
454 tubulin) visualised by immunolabelling using anti Glu-tubulin antibodies and
455 fluorescently-labelled secondary antibodies. Bars = 10 μ m. (D) Cells as in A
456 were lysed and lysates immunoblotted for acetylated- α -tubulin (Ac-tubulin)
457 and α -tubulin. (E) myc-SseJ production was induced in NRK cells up to 24h.
458 Lysates were generated and western blotted for myc-SseJ, acetylated-tubulin
459 and Rho (pan specific). (F) NRK cells (Ctrl) and those expressing sseJ (SseJ)
460 were transfected with a plasmid encoding EB3-tdTomato. EB3-tdTomato was

461 visualised live, 24h later, on a spinning disc confocal microscope. Images
462 represent a single time frame. Bars = 10 μ m.

463

464 **Figure 4. SseJ binds GTPases RhoA and RhoC.** (A) Anti-myc antibody was
465 covalently attached to sepharose and myc-SseJ was immunoprecipitated from
466 control (Ctrl) NRK cells or NRK cells expressing myc-SseJ (myc-SseJ).
467 Proteins bound to the beads were eluted and subjected to SDS-PAGE and
468 the gel stained with coomassie (shown). SseJ is indicated by an arrowhead. A
469 band at \approx 21kDa specifically found in the SseJ immunoprecipitation was
470 excised and sequenced by mass spectroscopy and identified both RhoA and
471 RhoC. Peptides identified are shown by the insert with peptides common to
472 both RhoA and RhoC shown in bold, peptides unique to RhoA shown in blue
473 and peptides unique to RhoC shown by red. Only a single peptide was unique
474 to RhoC (highlighted by an asterisk). (B) Experiments as shown in A,
475 including cells expressing myc-SseJ(S151A), were repeated and western
476 blotted for myc, RhoA and RhoC. Western blots show 1/10th of the input
477 before and after the immunoprecipitation and the total eluate from the
478 immunoprecipitations. (C) The activity of RhoA was measured by ELISA, on
479 extracts from control cells and cells expressing myc-SseJ or myc-SseJ
480 (S151A) mutant. Data are means \pm SD, n=8.

481

482 **References**

- 483 1. van der Heijden J, Finlay BB. Type III effector-mediated processes in
484 Salmonella infection. *Future microbiology*. 2012;7(6):685-703. doi:
485 10.2217/fmb.12.49. PubMed PMID: 22702524.
- 486 2. Garcia-del Portillo F, Finlay BB. Targeting of Salmonella typhimurium to
487 vesicles containing lysosomal membrane glycoproteins bypasses compartments
488 with mannose 6-phosphate receptors. *The Journal of cell biology*.
489 1995;129(1):81-97. PubMed PMID: 7698996; PubMed Central PMCID:
490 PMC2120372.
- 491 3. Drecktrah D, Knodler LA, Howe D, Steele-Mortimer O. Salmonella
492 trafficking is defined by continuous dynamic interactions with the
493 endolysosomal system. *Traffic*. 2007;8(3):212-25. doi: 10.1111/j.1600-
494 0854.2006.00529.x. PubMed PMID: 17233756; PubMed Central PMCID:
495 PMC2063589.
- 496 4. McGourty K, Thurston TL, Matthews SA, Pinaud L, Mota LJ, Holden DW.
497 Salmonella inhibits retrograde trafficking of mannose-6-phosphate receptors
498 and lysosome function. *Science*. 2012;338(6109):963-7. doi:
499 10.1126/science.1227037. PubMed PMID: 23162002.
- 500 5. Hernandez LD, Hueffer K, Wenk MR, Galan JE. Salmonella modulates
501 vesicular traffic by altering phosphoinositide metabolism. *Science*.
502 2004;304(5678):1805-7. doi: 10.1126/science.1098188. PubMed PMID:
503 15205533.
- 504 6. Fratti RA, Backer JM, Gruenberg J, Corvera S, Deretic V. Role of
505 phosphatidylinositol 3-kinase and Rab5 effectors in phagosomal biogenesis and
506 mycobacterial phagosome maturation arrest. *The Journal of cell biology*.
507 2001;154(3):631-44. doi: 10.1083/jcb.200106049. PubMed PMID: 11489920;
508 PubMed Central PMCID: PMC2196432.
- 509 7. Swanson J, Bushnell A, Silverstein SC. Tubular lysosome morphology and
510 distribution within macrophages depend on the integrity of cytoplasmic
511 microtubules. *Proceedings of the National Academy of Sciences of the United*
512 *States of America*. 1987;84(7):1921-5. PubMed PMID: 3550801; PubMed Central
513 PMCID: PMC304553.
- 514 8. Jahraus A, Storrie B, Griffiths G, Desjardins M. Evidence for retrograde
515 traffic between terminal lysosomes and the prelysosomal/late endosome
516 compartment. *Journal of cell science*. 1994;107 (Pt 1):145-57. PubMed PMID:
517 8175904.
- 518 9. Desjardins M, Huber LA, Parton RG, Griffiths G. Biogenesis of
519 phagolysosomes proceeds through a sequential series of interactions with the
520 endocytic apparatus. *The Journal of cell biology*. 1994;124(5):677-88. PubMed
521 PMID: 8120091; PubMed Central PMCID: PMC2119957.
- 522 10. Darsow T, Odorizzi G, Emr SD. Invertase fusion proteins for analysis of
523 protein trafficking in yeast. *Methods in enzymology*. 2000;327:95-106. PubMed
524 PMID: 11044977.
- 525 11. Shohdy N, Efe JA, Emr SD, Shuman HA. Pathogen effector protein
526 screening in yeast identifies Legionella factors that interfere with membrane
527 trafficking. *Proceedings of the National Academy of Sciences of the United States*
528 *of America*. 2005;102(13):4866-71. doi: 10.1073/pnas.0501315102. PubMed
529 PMID: 15781869; PubMed Central PMCID: PMC555709.
- 530 12. Thi EP, Hong CJ, Sanghera G, Reiner NE. Identification of the
531 Mycobacterium tuberculosis protein PE-PGRS62 as a novel effector that

532 functions to block phagosome maturation and inhibit iNOS expression. Cellular
533 microbiology. 2013;15(5):795-808. doi: 10.1111/cmi.12073. PubMed PMID:
534 23167250.

535 13. Raymond CK, Howald-Stevenson I, Vater CA, Stevens TH. Morphological
536 classification of the yeast vacuolar protein sorting mutants: evidence for a
537 prevacuolar compartment in class E vps mutants. Molecular biology of the cell.
538 1992;3(12):1389-402. PubMed PMID: 1493335; PubMed Central PMCID:
539 PMC275707.

540 14. Banta LM, Robinson JS, Klionsky DJ, Emr SD. Organelle assembly in yeast:
541 characterization of yeast mutants defective in vacuolar biogenesis and protein
542 sorting. The Journal of cell biology. 1988;107(4):1369-83. PubMed PMID:
543 3049619; PubMed Central PMCID: PMC2115260.

544 15. Miao EA, Miller SI. A conserved amino acid sequence directing
545 intracellular type III secretion by Salmonella typhimurium. Proceedings of the
546 National Academy of Sciences of the United States of America.
547 2000;97(13):7539-44. PubMed PMID: 10861017; PubMed Central PMCID:
548 PMC16581.

549 16. Figueira R, Watson KG, Holden DW, Helaine S. Identification of salmonella
550 pathogenicity island-2 type III secretion system effectors involved in
551 intramacrophage replication of S. enterica serovar typhimurium: implications for
552 rational vaccine design. mBio. 2013;4(2):e00065. doi: 10.1128/mBio.00065-13.
553 PubMed PMID: 23592259; PubMed Central PMCID: PMC3634603.

554 17. Freeman JA, Ohl ME, Miller SI. The Salmonella enterica serovar
555 typhimurium translocated effectors SseJ and SifB are targeted to the Salmonella-
556 containing vacuole. Infection and immunity. 2003;71(1):418-27. PubMed PMID:
557 12496192; PubMed Central PMCID: PMC143161.

558 18. Lawley TD, Chan K, Thompson LJ, Kim CC, Govoni GR, Monack DM.
559 Genome-wide screen for Salmonella genes required for long-term systemic
560 infection of the mouse. PLoS pathogens. 2006;2(2):e11. doi:
561 10.1371/journal.ppat.0020011. PubMed PMID: 16518469; PubMed Central
562 PMCID: PMC1383486.

563 19. Ruiz-Albert J, Yu XJ, Beuzon CR, Blakey AN, Galyov EE, Holden DW.
564 Complementary activities of SseJ and SifA regulate dynamics of the Salmonella
565 typhimurium vacuolar membrane. Molecular microbiology. 2002;44(3):645-61.
566 PubMed PMID: 11994148.

567 20. Matteoni R, Kreis TE. Translocation and clustering of endosomes and
568 lysosomes depends on microtubules. The Journal of cell biology.
569 1987;105(3):1253-65. PubMed PMID: 3308906; PubMed Central PMCID:
570 PMC2114818.

571 21. Upton C, Buckley JT. A new family of lipolytic enzymes? Trends in
572 biochemical sciences. 1995;20(5):178-9. PubMed PMID: 7610479.

573 22. Ohlson MB, Fluhr K, Birmingham CL, Brumell JH, Miller SI. SseJ deacylase
574 activity by Salmonella enterica serovar Typhimurium promotes virulence in mice.
575 Infection and immunity. 2005;73(10):6249-59. doi: 10.1128/IAI.73.10.6249-
576 6259.2005. PubMed PMID: 16177296; PubMed Central PMCID: PMC1230951.

577 23. Nawabi P, Catron DM, Haldar K. Esterification of cholesterol by a type III
578 secretion effector during intracellular Salmonella infection. Molecular
579 microbiology. 2008;68(1):173-85. doi: 10.1111/j.1365-2958.2008.06142.x.
580 PubMed PMID: 18333886.

- 581 24. Lossi NS, Rolhion N, Magee AI, Boyle C, Holden DW. The Salmonella SPI-2
582 effector SseJ exhibits eukaryotic activator-dependent phospholipase A and
583 glycerophospholipid : cholesterol acyltransferase activity. *Microbiology*.
584 2008;154(Pt 9):2680-8. doi: 10.1099/mic.0.2008/019075-0. PubMed PMID:
585 18757801; PubMed Central PMCID: PMC2885629.
- 586 25. Garcia-del Portillo F, Zwick MB, Leung KY, Finlay BB. Salmonella induces
587 the formation of filamentous structures containing lysosomal membrane
588 glycoproteins in epithelial cells. *Proceedings of the National Academy of Sciences*
589 *of the United States of America*. 1993;90(22):10544-8. PubMed PMID: 8248143;
590 PubMed Central PMCID: PMCPMC47813.
- 591 26. Khawaja S, Gundersen GG, Bulinski JC. Enhanced stability of microtubules
592 enriched in detyrosinated tubulin is not a direct function of detyrosination level.
593 *The Journal of cell biology*. 1988;106(1):141-9. PubMed PMID: 3276710;
594 PubMed Central PMCID: PMC2114950.
- 595 27. Palazzo A, Ackerman B, Gundersen GG. Cell biology: Tubulin acetylation
596 and cell motility. *Nature*. 2003;421(6920):230. doi: 10.1038/421230a. PubMed
597 PMID: 12529632.
- 598 28. Li W, Zhao Y, Chou IN. Alterations in cytoskeletal protein sulfhydryls and
599 cellular glutathione in cultured cells exposed to cadmium and nickel ions.
600 *Toxicology*. 1993;77(1-2):65-79. PubMed PMID: 8442019.
- 601 29. Ledda FD, Ramoino P, Ravera S, Perino E, Bianchini P, Diaspro A, et al.
602 Tubulin posttranslational modifications induced by cadmium in the sponge
603 *Clathrina clathrus*. *Aquatic toxicology*. 2013;140-141:98-105. doi:
604 10.1016/j.aquatox.2013.05.013. PubMed PMID: 23765032.
- 605 30. Hodge RG, Ridley AJ. Regulating Rho GTPases and their regulators. *Nature*
606 *reviews Molecular cell biology*. 2016;17(8):496-510. doi: 10.1038/nrm.2016.67.
607 PubMed PMID: 27301673.
- 608 31. Ohlson MB, Huang Z, Alto NM, Blanc MP, Dixon JE, Chai J, et al. Structure
609 and function of Salmonella SifA indicate that its interactions with SKIP, SseJ, and
610 RhoA family GTPases induce endosomal tubulation. *Cell host & microbe*.
611 2008;4(5):434-46. doi: 10.1016/j.chom.2008.08.012. PubMed PMID: 18996344;
612 PubMed Central PMCID: PMC2658612.
- 613 32. Christen M, Coye LH, Hontz JS, LaRock DL, Pfuetzner RA, Megha, et al.
614 Activation of a bacterial virulence protein by the GTPase RhoA. *Science signaling*.
615 2009;2(95):ra71. doi: 10.1126/scisignal.2000430. PubMed PMID: 19887681.
- 616 33. Kolodziejek AM, Miller SI. Salmonella modulation of the phagosome
617 membrane, role of SseJ. *Cellular microbiology*. 2015;17(3):333-41. doi:
618 10.1111/cmi.12420. PubMed PMID: 25620407.
- 619 34. Palazzo AF, Cook TA, Alberts AS, Gundersen GG. mDia mediates Rho-
620 regulated formation and orientation of stable microtubules. *Nature cell biology*.
621 2001;3(8):723-9. doi: 10.1038/35087035. PubMed PMID: 11483957.
- 622 35. Wheeler AP, Ridley AJ. Why three Rho proteins? RhoA, RhoB, RhoC, and
623 cell motility. *Experimental cell research*. 2004;301(1):43-9. doi:
624 10.1016/j.yexcr.2004.08.012. PubMed PMID: 15501444.
- 625 36. Dehmelt L, Halpain S. The MAP2/Tau family of microtubule-associated
626 proteins. *Genome biology*. 2005;6(1):204. doi: 10.1186/gb-2004-6-1-204.
627 PubMed PMID: 15642108; PubMed Central PMCID: PMC549057.
- 628 37. Castro-Alvarez JF, Gutierrez-Vargas J, Darnaudery M, Cardona-Gomez GP.
629 ROCK inhibition prevents tau hyperphosphorylation and p25/CDK5 increase

630 after global cerebral ischemia. Behavioral neuroscience. 2011;125(3):465-72.
631 doi: 10.1037/a0023167. PubMed PMID: 21517148.

632 38. Pan J, Lordier L, Meyran D, Rameau P, Lecluse Y, Kitchen-Goosen S, et al.
633 The formin DIAPH1 (mDia1) regulates megakaryocyte proplatelet formation by
634 remodeling the actin and microtubule cytoskeletons. Blood. 2014;124(26):3967-
635 77. doi: 10.1182/blood-2013-12-544924. PubMed PMID: 25298036.

636 39. Harrison RE, Bucci C, Vieira OV, Schroer TA, Grinstein S. Phagosomes fuse
637 with late endosomes and/or lysosomes by extension of membrane protrusions
638 along microtubules: role of Rab7 and RILP. Molecular and cellular biology.
639 2003;23(18):6494-506. PubMed PMID: 12944476; PubMed Central PMCID:
640 PMC193691.

641 40. Brumell JH, Tang P, Mills SD, Finlay BB. Characterization of Salmonella-
642 induced filaments (Sifs) reveals a delayed interaction between Salmonella-
643 containing vacuoles and late endocytic compartments. Traffic. 2001;2(9):643-53.
644 PubMed PMID: 11555418.

645 41. Stein MA, Leung KY, Zwick M, Garcia-del Portillo F, Finlay BB.
646 Identification of a Salmonella virulence gene required for formation of
647 filamentous structures containing lysosomal membrane glycoproteins within
648 epithelial cells. Molecular microbiology. 1996;20(1):151-64. PubMed PMID:
649 8861213.

650 42. Rajashekar R, Liebl D, Seitz A, Hensel M. Dynamic remodeling of the
651 endosomal system during formation of Salmonella-induced filaments by
652 intracellular Salmonella enterica. Traffic. 2008;9(12):2100-16. doi:
653 10.1111/j.1600-0854.2008.00821.x. PubMed PMID: 18817527.

654 43. Birmingham CL, Jiang X, Ohlson MB, Miller SI, Brumell JH. Salmonella-
655 induced filament formation is a dynamic phenotype induced by rapidly
656 replicating Salmonella enterica serovar typhimurium in epithelial cells. Infection
657 and immunity. 2005;73(2):1204-8. doi: 10.1128/IAI.73.2.1204-1208.2005.
658 PubMed PMID: 15664965; PubMed Central PMCID: PMC547014.

659 44. Robinson JM, Okada T, Castellot JJ, Jr., Karnovsky MJ. Unusual lysosomes
660 in aortic smooth muscle cells: presence in living and rapidly frozen cells. The
661 Journal of cell biology. 1986;102(5):1615-22. PubMed PMID: 3700469; PubMed
662 Central PMCID: PMC2114221.

663 45. Swanson JA, Yirinec BD, Silverstein SC. Phorbol esters and horseradish
664 peroxidase stimulate pinocytosis and redirect the flow of pinocytosed fluid in
665 macrophages. The Journal of cell biology. 1985;100(3):851-9. PubMed PMID:
666 3972898; PubMed Central PMCID: PMC2113515.

667 46. Phaire-Washington L, Silverstein SC, Wang E. Phorbol myristate acetate
668 stimulates microtubule and 10-nm filament extension and lysosome
669 redistribution in mouse macrophages. The Journal of cell biology.
670 1980;86(2):641-55. PubMed PMID: 6893202; PubMed Central PMCID:
671 PMC2111499.

672 47. Bright NA, Gratian MJ, Luzio JP. Endocytic delivery to lysosomes mediated
673 by concurrent fusion and kissing events in living cells. Current biology : CB.
674 2005;15(4):360-5. doi: 10.1016/j.cub.2005.01.049. PubMed PMID: 15723798.

675 48. McMahon HT, Kozlov MM, Martens S. Membrane curvature in synaptic
676 vesicle fusion and beyond. Cell. 2010;140(5):601-5. doi:
677 10.1016/j.cell.2010.02.017. PubMed PMID: 20211126.

- 678 49. Lemichez E, Aktories K. Hijacking of Rho GTPases during bacterial
679 infection. *Experimental cell research*. 2013;319(15):2329-36. doi:
680 10.1016/j.yexcr.2013.04.021. PubMed PMID: 23648569.
- 681 50. Quintero CA, Tudela JG, Damiani MT. Rho GTPases as pathogen targets:
682 Focus on curable sexually transmitted infections. *Small GTPases*. 2015;6(2):108-
683 18. doi: 10.4161/21541248.2014.991233. PubMed PMID: 26023809.
- 684 51. Horazdovsky BF, Busch GR, Emr SD. VPS21 encodes a rab5-like GTP
685 binding protein that is required for the sorting of yeast vacuolar proteins. *The*
686 *EMBO journal*. 1994;13(6):1297-309. PubMed PMID: 8137814; PubMed Central
687 PMCID: PMC394945.
- 688 52. Wilson K. Preparation of genomic DNA from bacteria. *Current protocols in*
689 *molecular biology* / edited by Frederick M Ausubel [et al]. 2001;Chapter 2:Unit 2
690 4. doi: 10.1002/0471142727.mb0204s56. PubMed PMID: 18265184.
- 691 53. Vernet T, Dignard D, Thomas DY. A family of yeast expression vectors
692 containing the phage f1 intergenic region. *Gene*. 1987;52(2-3):225-33. PubMed
693 PMID: 3038686.
- 694 54. Girotti M, Banting G. TGN38-green fluorescent protein hybrid proteins
695 expressed in stably transfected eukaryotic cells provide a tool for the real-time,
696 in vivo study of membrane traffic pathways and suggest a possible role for
697 ratTGN38. *Journal of cell science*. 1996;109 (Pt 12):2915-26. PubMed PMID:
698 9013339.
- 699 55. Gietz RD, Schiestl RH. Transforming yeast with DNA. *Method Mol Cell Biol*.
700 1995;5(5):255-69. PubMed PMID: WOS:A1995UH90700003.

701

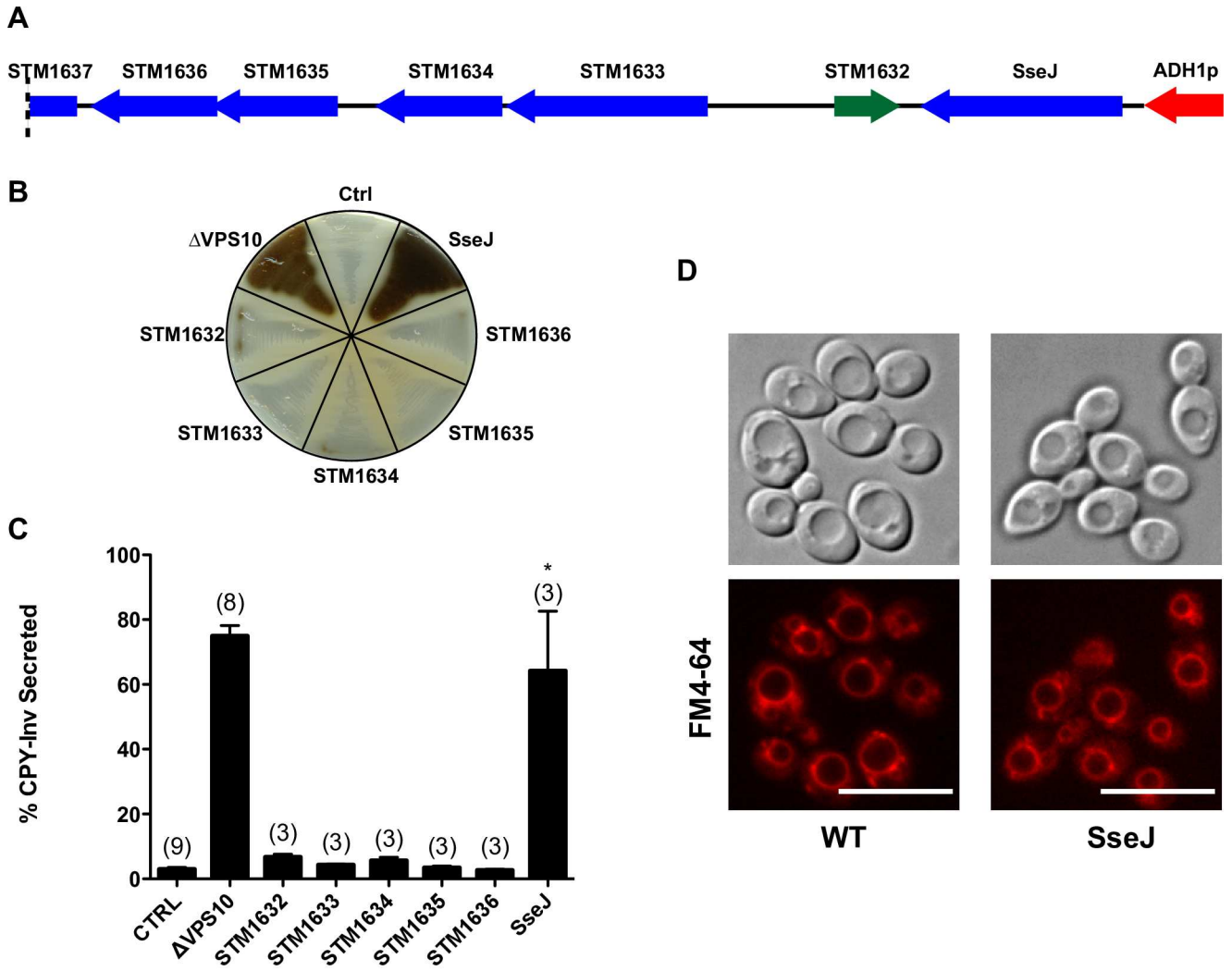


Fig 1

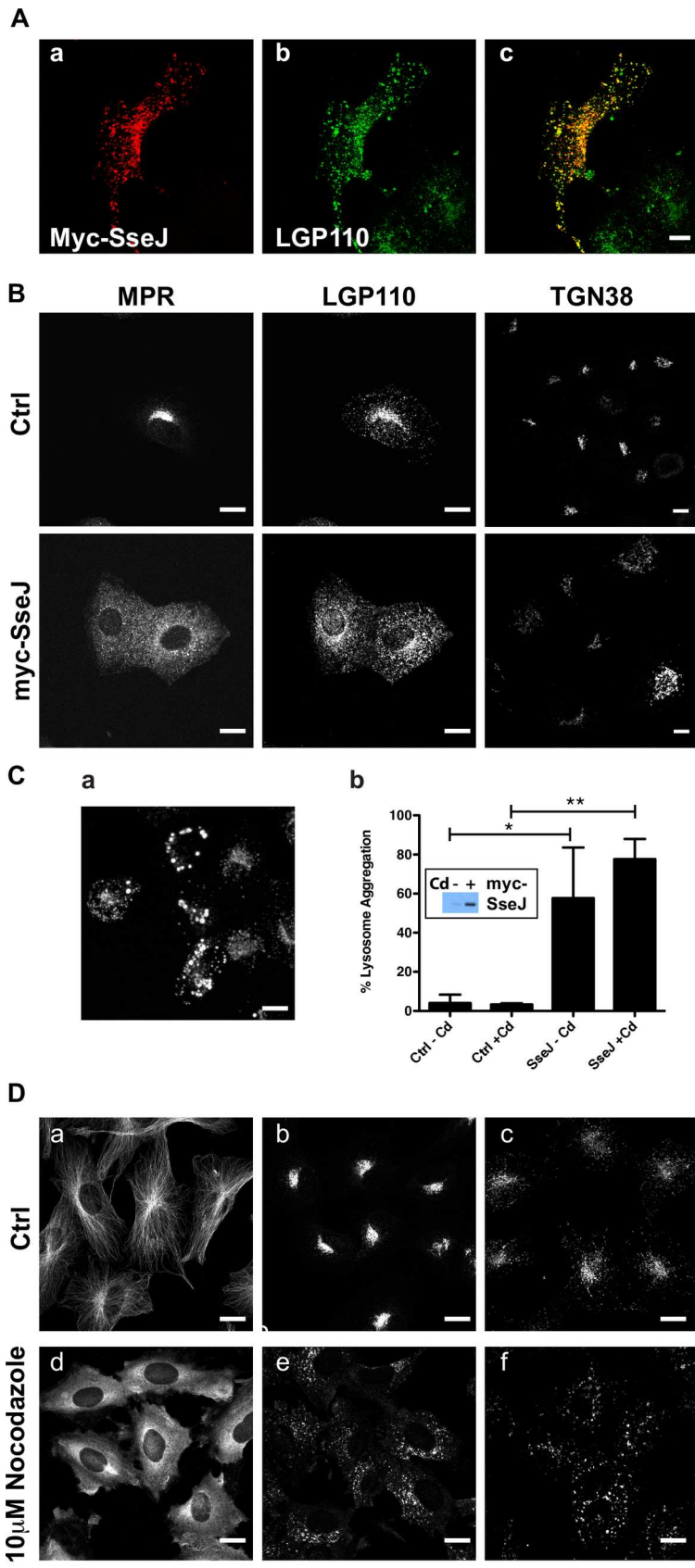


Fig 2

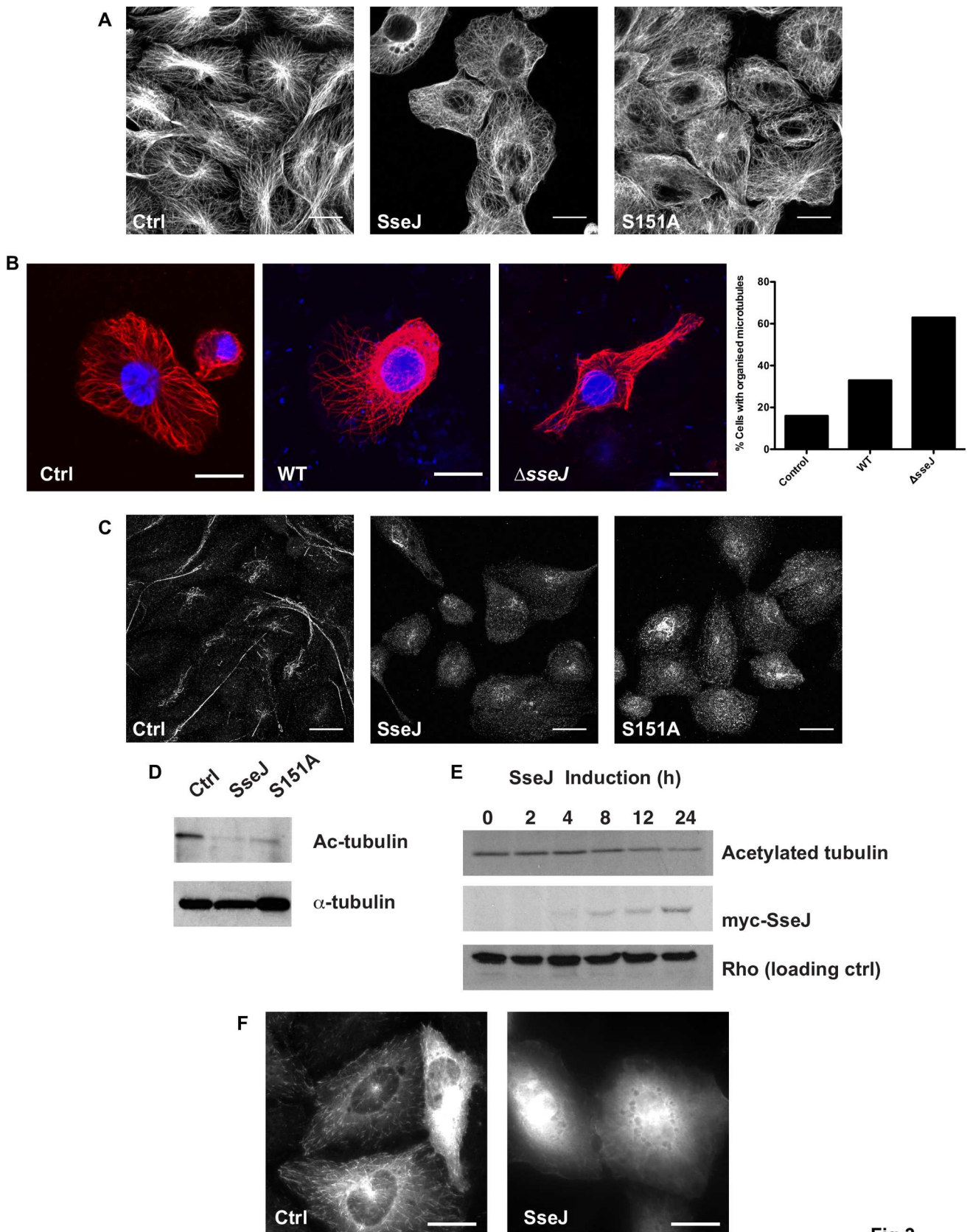
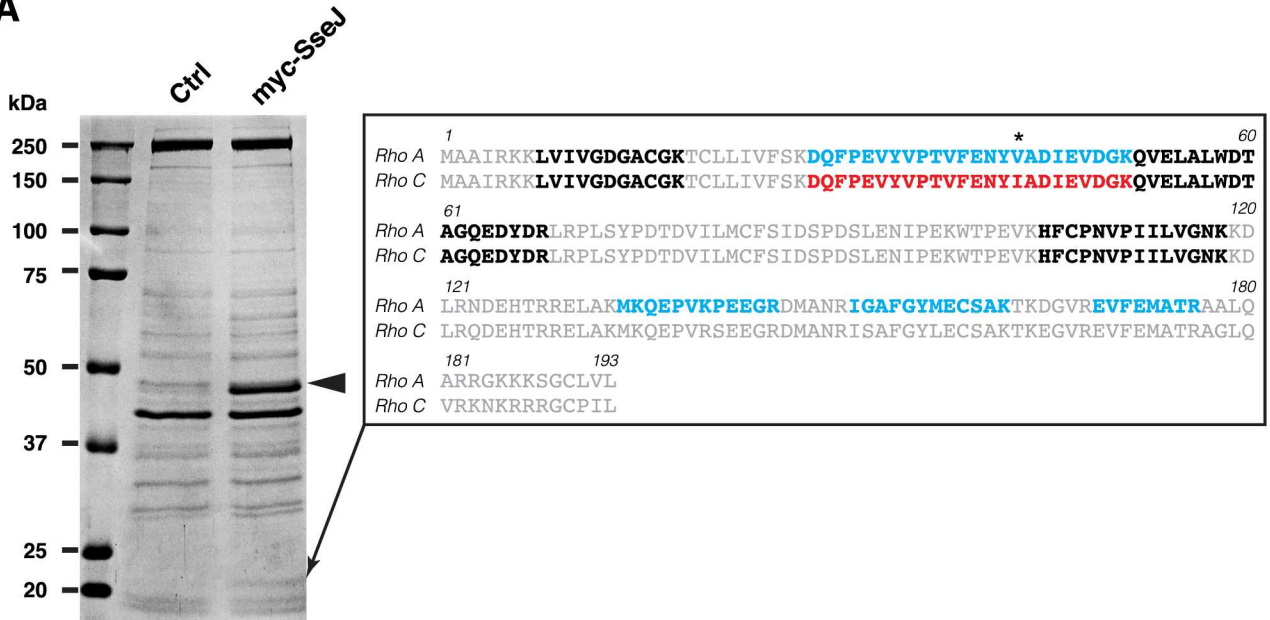
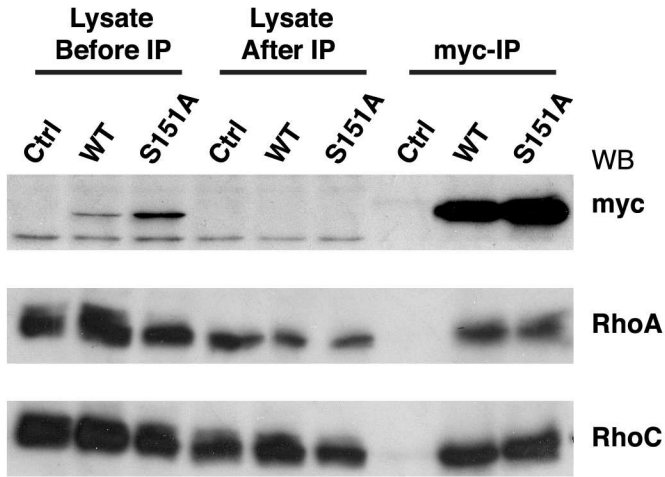


Fig 3

A



B



C

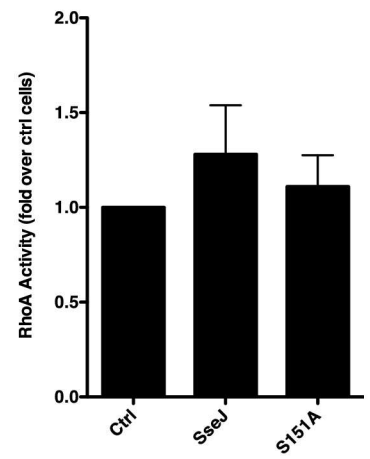


Fig 4